https://doi.org/10.2352/CIC.2024.32.1.19

Large Size of Color Constancy: Enhancing Pure Color Image Illuminant Estimation with Kolmogorov-Arnold Networks

***LiangWei Chen*[1] *, Ming Ronnier Luo*[1*] *, MinChen Wei*[2]**
[1] ***State Key Laboratory of Extreme Photonics and Instrumentation, Zhejiang University, Hangzhou, China.***
[2] ***Color, Imaging, and Illumination Laboratory, The Hong Kong Polytechnic University, Kowloon, Hong Kong, China***
****Corresponding author: Ming Ronnier Luo, m.r.luo@zju.edu.cn***

Abstract

Large efforts have been made to perform illuminant estimation, resulting in the development of various statistical- and learning-based methods. However, there have been challenges for some types of images, such as a single color, referred to as pure color images, which is the focus of the present research.. In this study, the neural network approach is used. It was found the Kolmogorov-Arnold Networks (KAN) model, a novel approach that diverges from traditional Multi-Layer Perceptron (MLP) architectures gave the accurate predictions. Our method, "Large Size Colour Constancy" (LSCC), characterized by its unique neural network structure, achieves high accuracy in illuminant estimation with significantly fewer parameters and enhanced interpretability. Additionally, three new pure color image datasets—"ZJU Color Fabric", "ZJU 0.8 Real Scene", and "ZJU 1.0 Real Scene" were produced—covering a wide range of conditions, including indoor and outdoor environments, as well as natural and artificial light sources. The results showed LSCC method to outperform existing methods across not only the pure colour datasets but also the traditional datasets, including classical normal images. It should offers practical deployment potential due to its efficiency and reduced computational requirements.

Introduction

In the field of computational color constancy, the focus is to adjust the colors in an image to appear as they would under a standard illuminant, effectively removing any color cast caused by varying lighting conditions. This process is analogous to the auto white balance function in modern digital cameras, including those in smartphones, and is a critical step in the image signal processing pipeline to ensure high-quality images. Various methods have been developed to estimate the illuminant in captured images, ranging from statistical approaches to learning-based techniques.

Traditional statistical methods often rely on assumptions about the statistical properties of colors in an image, such as those employed in the grey world [1], white patch [2], shades of grey [3], and PCA-based [4] methods. Although these methods are computationally efficient, their underlying assumptions frequently do not hold in real-world scenarios. Consequently, these methods often result in inaccurate illuminant estimation and poor image quality, particularly in scenes dominated by a single color, referred to as pure color images.

Recent advancements in neural networks have enhanced learning-based methods for color constancy. The Pure Color Constancy (PCC) method [5], for example, improves illuminant estimation accuracy for pure color images through representative color inputs and a lightweight network design. However, PCC, like other methods based on Multi-Layer Perceptrons (MLPs), CNNs, RNNs, and Transformers, faces inherent limitations due to its underlying architecture despite increasing structural complexity.

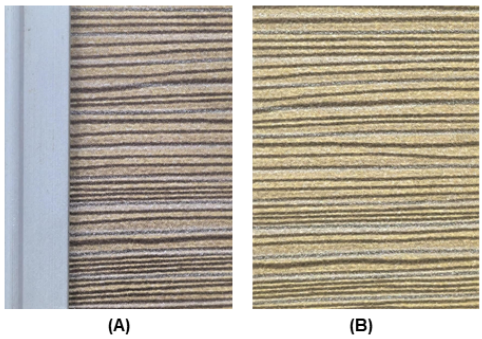

Figure 1. *Examples of real-world pure color scenes captured using a smartphone. (A) is an image taken with additional reference colors present in the scene, while (B) is a pure color image without any other reference colors. (B) was taken by shifting the smartphone slightly to the right after capturing (A), ensuring that both images were taken under the same lighting conditions.*

To overcome these limitations, the present work proposes a novel method—Large Size Colour Constancy (LSCC), introducing Kolmogorov-Arnold Networks (KAN) to automatic white balance for the first time. KAN's novel architecture diverges from traditional MLP-based methods, significantly reducing parameters while enhancing prediction accuracy and interpretability. LSCC outperforms existing methods in various real-world conditions, including pure color and complex scenes, setting a new benchmark in computational color constancy.

Pure or large size, color images, dominated by a single color, lack the semantic information needed for accurate illuminant estimation. These images are common, especially with advancements in smartphone macro and telephoto photography, often leading to incorrect white balance (Figure 1). Despite their prevalence, existing methods have not been extensively tested on pure color images due to their unique characteristics and the lack of dedicated datasets. This gap has limited research in this area.

With the above in mind, three novel pure color image datasets: "ZJU Color Fabric" (ZJU-CF), "ZJU 0.8 Real Scene"(ZJU-0.8RS), and "ZJU 1.0 Real Scene" (ZJU-1.0RS)dataset, captured using mirrorless interchangeable lens

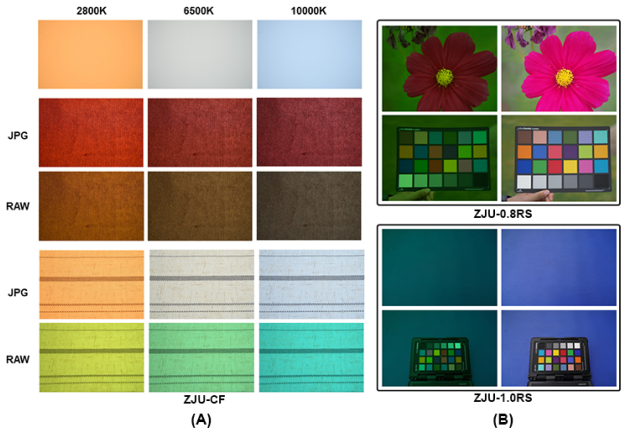

Figure 2. *(A) an example of two different fabric textures included in the "ZJU Color Fabric" dataset. Top row is JPG images of gray card, the second and the third row is JPG images and RAW images of one of the textured fabrics, the bottom two row is another one. Left column, images taken under 2800K color temperature light source, 6500K and 10000K to the right. (B) an example of an image from each of the two datasets. Top row are images without color checker; bottom row are images with color checker; left column are RAW images; right column are JPG images. The top part is an example image from the ZJU-0.8RS dataset and the bottom part is an example image from the ZJU-1.0RS dataset.*

camera (MILC) were produced. They include various examples of pure color scenes, covering a variety of conditions containing indoor and outdoor environments, as well as natural and artificial light sources, offering a comprehensive resource for evaluating color constancy methods under these challenging conditions.

"ZJU Pure Color" Image Dataset

Existing Datasets for Illumination Estimation

Several image datasets are widely utilized in various research areas to study illumination estimation, including the ColorChecker [6], NUS-8 [4], Cube+ [8], etc. and the first dataset of pure color scenes, "PolyU Pure Color" dataset [5]. Table 1 summarises the information of these datasets, including dataset size and color temperature distribution information, etc. It should be noted that the ColorChecker dataset was the latest Recommended Color Checker (CC2018) dataset with improved ground-truth illuminants [9].

The PolyU Pure Color image dataset specifically includes pure color images from both outdoor scenes (e.g., green grass, blue sky, and flowers) and indoor scenes (e.g., illuminated fabrics and walls). Despite its smaller size compared to other datasets, it provides valuable data for research on pure color images. It is of great help to industrial research. However, there is still lack of pure color images captured using advanced cameras.

"ZJU Color Fabric" Dataset

The "ZJU Color Fabric" dataset (ZJU-CF) was captured in LED Cube, which can generate light sources based on CCT, Duv or spectrum, controlled by computer software. The dataset contains images of 144 pieces of fabric include different color and different texture, under 16 color temperature light sources (e.g., 2800K, 3000, 3500K, 4000K, 4500K, 5000K, 5500K, 6000K, 6500K, 7000K, 7500K, 8000K, 8500K, 9000K, 9500K, 10000K). All images were taken with fixed settings, and other information is shown in table 1. The images were processed by dcraw, with manual white balance, then uniform correction is performed based on the gray card taken in advance. The gray card images are shown at the top of Figure 2(A).

Before capturing the images, all 16 light sources were set up and stored in the LED Cube control device. All light sources are measured by Jeti to ensure that the Duv value is less than 0.003. During the image capture process, the camera was set to automatically shoot every 3 seconds and the control device of the LED Cube was clicked to switch the light source during the shooting interval, which effectively avoided the camera shake caused by pressing the shutter.

After processing, the images were saved in NPY format for Python reading. The middle two rows and the bottom two rows of Figure 2(A) show images of two different fabrics taken under light sources with color temperatures of 2800K, 6500K, and 10000K. Then an image is divided into a 3x3 grid of nine segments, which serves as a data augmentation.

"ZJU 0.8/1.0 Real Scene" Dataset

The "ZJU 0.8 Real Scene" dataset (ZJU-0.8RS) and "ZJU 1.0 Real Scene" dataset (ZJU-1.0RS) were both extensions of the pure color images dataset, including outdoor scenes and indoor scenes. ZJU-0.8RS under 39 different light source scenes, ZJU-1.0RS contain 49 outdoor and 40 indoor images and other information about the two datasets is summarized in Table 1.

Before capturing each image of ZJU-0.8RS, a ColorChecker facing the light source will be captured first, allowing the collection of the ground-truth illuminant in the scene. A CL500A spectroradiometer was also used to collect the ground-truth illuminant in the scene, contain the XYZ, color temperature, Duv, spectrum and other information of light source. Then the image in this scene should be collected as soon as possible to avoid inaccurate ground-truth illuminant caused by changes in outdoor light sources.

When capturing each image in ZJU-1.0 RS dataset, an X-Rite ColorChecker placed in the scene was captured, the ground-truth illuminant was then calculated using the rgb values of the "white" patch in the ColorChecker target, and the normalized rgb values were saved in NPY file in a folder different from the image, with the same file name as the image, so that the images can be processed directly without masking the color checkers. Both the images with and without the ColorChecker were also saved in a JPG format, which was processed by the camera automatically for visualization and all processes above are also applied to the ZJU-0.8RS dataset. Figure 2(b) shows an image from each of the two datasets, including the RAW images with and without the color checker and the JPG images for visualization.

Table1: Summary of the datasets used in the study, and M means MILC, D means DSLR

Datasets	No. of original	No. after augmentation	Device Used	Type	CCT Range / Mode / The proportion of the majority
Poly-U	102	4529	Smartphone (Huawei P50 Pro)	Pure color	3000K-8000K / 7000K / 37.25%
ZJU-CF	2304	23231	M (Nikon Z6)	Pure color	2800K - 10000K / (Artificial)
ZJU 0.8RS	214	5469	M (Olympus E-M1 mark ii)	Pure color	2500K-6500K / 5500K / 48.22%
ZJU 1.0RS	90	5875	M (Sony a7r4)	Pure color	2000K-7000K / 3000 / 27.78%
CC2018	568	-	D (Canon 1D and 5D)	Classical	3500K-8500K / 5000K / 35.56%
NUS-8	210*8	-	D (8 cameras)	Classical	3000K-8500K / 5000K / 37.11%
Cube+	1707	-	D (Canon EOS 550D)	Classical	2500K-8500K / 4500K / 43.29%

Proposed "Large Size Colour Constancy" Method

Related Work

To address the white balance issue in pure color scenes, Yue et al. first proposed the PCC method [5], which combines four color inputs with a neural network, achieving notable results. Inspired by feature-based methods, particularly Cheng et al.'s approach [4], the PCC method uses four color inputs: (1) normalized max chromaticities: the chromaticities of the maximal RGB values in each channel; (2) normalized mean chromaticities: the chromaticities of the mean RGB values in each channel; (3) normalized brightest chromaticities: the chromaticities of the pixel with the largest R + G + B value; (4) normalized darkest chromaticities: the chromaticities of the pixel with the smallest R + G + B value. These inputs have been shown in the paper [5] to effectively represent scene light sources. These four sets of chromaticities serve as inputs for a lightweight multilayer perceptron (MLP) neural network inspired by [7], with the structure shown in Figure 3(A).

MLP are fundamental components in contemporary deep learning architectures, yet they exhibit several inherent weaknesses that limit their effectiveness. MLP require a substantial number of parameters to accurately represent complex functions, resulting in significant computational costs and memory demands. Additionally, MLP employ global activation functions, leading to widespread propagation of local changes across the entire network. This characteristic often disrupts previously learned information, making MLP susceptible to catastrophic forgetting during continuous learning tasks. Furthermore, MLP are less efficient than splines in optimizing low-dimensional functions, as they struggle to precisely adjust univariate functions. Although MLP are capable of learning features, they are inefficient in approximating univariate functions, thus constraining their overall expressive power. From CNN, RNN, Transformer to the recent large models, although the structure is becoming more and more complex, they are all constantly modified on the neural network composed of MLP. Therefore, they also have same problems with MLP.

Not long ago, Liu et al. [11] proposed the Kolmogorov-Arnold Networks (KANs) model, address these weaknesses through innovative design principles that significantly enhance their flexibility and adaptability. Unlike MLPs, KANs utilize learnable activation functions on the edges (weights) rather than fixed activation functions on the nodes (neurons). This replacement of linear weight matrices with learnable univariate functions, parametrized as splines, allows KANs to adapt more effectively to complex tasks. The local nature of spline basis functions mitigates the issue of catastrophic forgetting, as any given sample only influences a limited set of spline coefficients, preserving the integrity of distant coefficients. This local adaptability ensures that learning new tasks does not degrade performance on previously learned tasks. Moreover, KANs typically require smaller network sizes than MLPs, which conserves computational resources and facilitates better universality and interpretability. By integrating the feature learning capabilities of MLPs with the precise univariate function optimization of splines, KANs effectively learn and optimize complex features with high accuracy, significantly enhancing their overall expressive power.

"Large Size Colour Constancy" Method

The proposed LSCC method includes a novel architecture to process chromaticity inputs for image analysis, offering significant improvements in performance and efficiency over traditional MLP-based learning methods, inspired by the above new KAN model. As illustrated in Figure 3(B), the structure comprises a series of fully connected layers, each utilizing learnable activation functions parameterized as splines rather than fixed nonlinearities at the nodes.

The method begins with an input layer with 8 nodes, representing the four chromaticity inputs extracted from the image. Since the four chromaticity inputs proposed by [5](e.g. normalized maximal, mean, brightest, and darkest pixel values) were proved that they are likely to vary under different illuminants, which are considered as four important inputs for estimating the illuminant, our method was still designed to use these four color inputs.

These inputs are then processed through multiple hidden layers with 9 nodes, where the learnable activation functions facilitate a more granular and locally adaptive transformation of the data. This configuration ensures that the network can capture complex patterns and relationships within the chromaticity space more effectively.

The output layer in $\mathbb{R}^2$ generates a set of estimated chromaticities ($\hat{r}$, $\hat{g}$), and the final chromaticity ($\hat{b}$) is computed as $1-\hat{r}-\hat{g}$, just like PCC. This approach not only provides a more accurate estimation of the chromaticity values but also ensures that the sum of the chromaticities adheres to the inherent constraints of the color space.

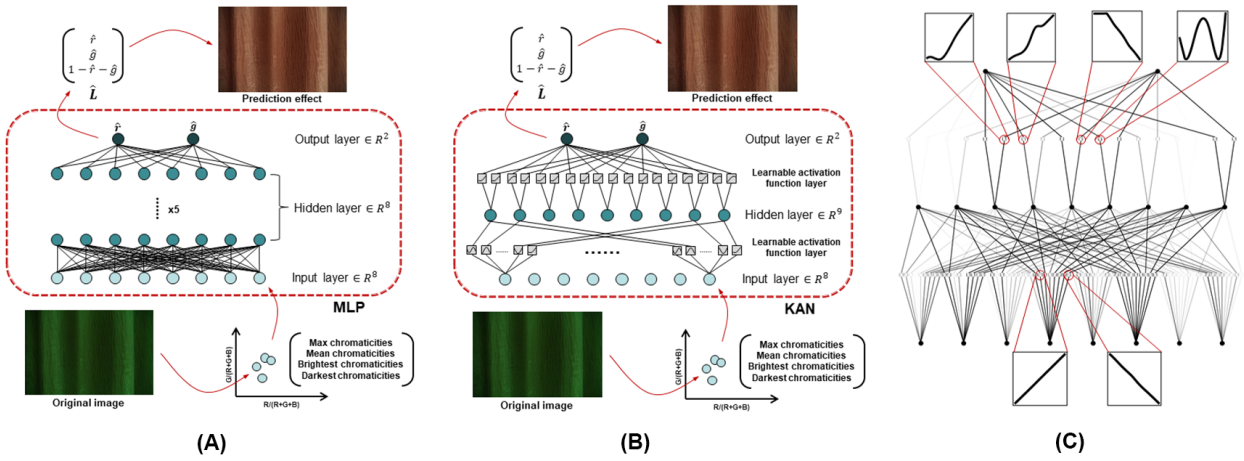

Figure 3. *(A) is the overview of the PCC method, and (B) is the overview of the LSCC method. Both two method, with the four color inputs, in terms of the normalized chromaticities, as the inputs for the neural network, and predicts a set of 2D ($\hat{r}$, $\hat{g}$) chromaticities as the estimated illuminant $\hat{L}$. (C) shows a trained LSCC model.*

Experiment and Results

Settings

The network was trained in PyTorch [12], and L-BFGS. Both was adopted as the optimization algorithm, with an overall penalty strength of 10^{-3} and an entropy penalty strength of 10. The batch size was set to 1, and the model with the best performance through a total of 2000 (for all the datasets), greatly reduced compared to MLP-based learning method, while ensuring the high accuracy. The order of the B-spline function k is set to 3, the number of grid intervals is also 3, and the angular error was adopted as the residual function and loss function. The standard angular error between the estimated and ground-truth illuminants, as calculated using Eq. 1.

$$\text{Angular Error} = \frac{180}{\pi} \arccos\left(\frac{\hat{L}\cdot L}{\|\hat{L}\|\cdot\|L\|}\right) \tag{1}$$

where $\hat{L}$ is the estimated illuminant and L is the ground-truth illuminant.

Data Augmentation and Pre-Processing

Although the proposed dataset contains relatively fewer images compared to other existing datasets such as NUS and Cube+, the AWB-Aug method [5] provides an effective means of data augmentation. This approach involves multiplying the original image I_0 by a 3×3 diagonal matrix M, with diagonal elements defined as $\left[\frac{r_a}{r_o}, \frac{g_a}{g_o}, \frac{b_a}{b_o}\right]$, where r_a, g_a, and b_a denote the augmented RGB values, and r_o, g_o, and b_o correspond to the original values. Initially, the augmentation process was carried out by randomly assigning RGB values within the range of 0.6 to 1.4, potentially resulting in illuminants that do not exist in reality. To address this, a subsequent augmentation step was performed, where RGB values were randomly assigned, ensuring that the chromaticity distance to the selected illuminants remained below 0.01.

All datasets used were processed into 16-bit PNG images by dcraw with the longest edge resized to 256 pixels, except for the PolyU dataset, which is 128×128 pixels and 8-bit format.

Network Design

Unlike MLP-based learning models, KAN models do not require a large number of parameters. However, an appropriate number of hidden layer nodes can significantly reduce training time and improve accuracy. Mathematically, the number of hidden layer nodes is generally less than 2n+1 [11], where n is the number of input nodes. In order to find the best number of hidden layer nodes, the ZJU-1.0RS dataset was employed as an example and test the number of hidden layer nodes from 4 to 19. Each number of nodes was tested 10 rounds. In each round of testing, 90% of the data was randomly selected as the training set, and the remaining 10% was the test set (note: 0.9/0.1 was proven to be the most robust split ratio in this scale of dataset). The test angular error and training time of each round were recorded, and the average value of 10 rounds was taken as the result of changing the number of hidden layer nodes, summarized in Figure 4.

It showed that the performance of LSCC does not increase with more parameters and take longer to train, like MLP-based

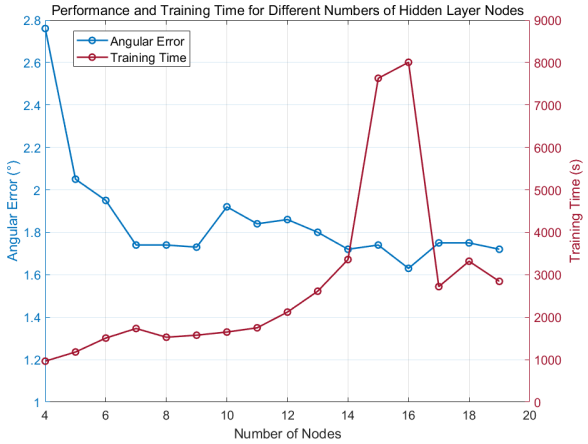

Figure 4. *Performance and training time for different numbers of hidden layer nodes.*

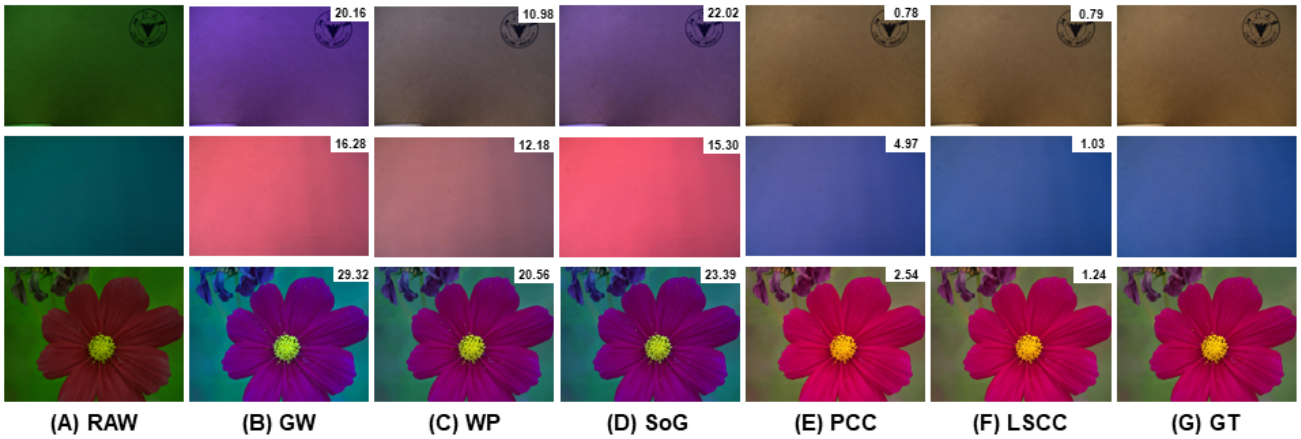

Figure 5. *Examples of the images in the "ZJU-0.8RS" and "ZJU-1.0RS" dataset. Column (A) shows the raw image, columns (B) to (E) show the images that were white balanced result estimated by the existing methods, follow by gray world (GW), white patch (WP), shade of grey (SoG) and PCC, column (F) shows the image that was white balanced using the estimated illuminant derived using the proposed LSCC method, and column (G) shows the image that was white balanced using the ground-truth illuminant. The angular error between the estimated and ground-truth illuminants is shown on the right top of each image.*

learning method. It is interesting that when the number of hidden layer nodes reaches 10, the model performance deteriorates, and when the number reaches 15 and 16, the training time becomes abnormally long and then suddenly decreased. This indicates that an inappropriate number of nodes will lead to poor model performance for the KAN model, because it will also apply pruning operations during the training process, and redundant nodes will only reduce node utilization efficiency and increase time consumption.

Figure 3(c) shows the trained network structure. It can be seen that many lines have faded or even disappeared. These faded or disappeared lines are the result of pruning, i.e. the smaller corresponding weight, the more serious line fades. This operation greatly improves the utilization rate of nodes and also reduces the size of the model. Zooming in on a portion of the trained activation functions, It can be seen that in addition to the linear relationship, each activation function is different, include some complex activation functions. This is why the KAN model can make accurate predictions with very few parameters. From the network structure, the weight of each chromaticity input and its relationship with the output can be further analysed, making the model more interpretable than MLP.

It was also found the multi-layer KAN model's performance did not improve much and the complexity and training increased exponentially. So, the proposed network illustrated in Figure 3(b) can achieve the best performance.

Results

The performance of the proposed method on pure color images in the ZJU-combined dataset (extracted from "ZJU-CF", "ZJU-0.8RS", and "ZJU-1.0RS") was compared with statistical and state-of-the-art learning-based methods. Table 2 summarizes the performance in terms of angular error, including mean, median (Med), trimean (Tri), best 25%, and worst 25%, with example images shown in Figure 5. To verify the universality, the PolyU dataset was used for training and the results were compared with those in [5] and Table 3 summarises the results of the methods' performance.. Additionally, cross-dataset predictions were performed where the model trained on the ZJU-combined dataset was used to predict illuminants for the individual datasets (ZJU-CF, ZJU-0.8RS, and ZJU-1.0RS) as well as the PolyU dataset. Table 4 summarises the results of the methods' performance.

In addition to pure color images, it is also important to evaluate the proposed KAN method using traditional normal images. For this purpose, the NUS-8 dataset for training and the Cube+ dataset for testing was applied. Table 5 summarizes the angular errors derived using various methods on these two datasets. For the NUS-8 dataset, the proposed KAN model was trained and evaluated on the images captured by Canon1DsMklll.

From Table 2 and 3, it can be observed that the statistical-

Table2: Summary of the performance of various statistical and learning-Based Methods, on the ZJU-combined datasets.

Method	Mean	Med.	Tri.	Best25%	Worst25%
GW	13.92	12.58	13.19	4.75	24.77
WP	12.71	11.95	12.20	6.03	20.74
SoG($p=6$)	11.11	9.70	10.17	3.42	21.24
C5 [10]	2.88	2.31	2.39	0.69	5.73
PCC	3.46	1.68	1.95	0.54	8.99
LSCC	2.40	1.56	1.77	0.44	5.53

Table3: Summary of the performance of various statistical- and learning-Based Methods on the PolyU dataset

Method	Mean	Med.	Tri.	Best25%	Worst25%
GW	10.37	8.14	8.67	2.60	21.40
WP	9.64	8.78	8.93	2.78	17.25
SoG($p=3$)	9.66	8.03	8.13	2.38	19.92
FFCC	3.56	1.97	3.05	0.58	9.39
C5	3.22	2.06	2.57	0.65	7.29
PCC	3.23	1.40	1.86	0.48	8.76
LSCC	2.52	1.36	1.38	0.38	7.67

Table4: Summary of the performance comparison between PCC and LSCC under cross-dataset prediction scenarios. The training dataset is "ZJU-combined"; values in parentheses indicate performance when using the prediction dataset on itself.

	PCC				LSCC			
Methods	**ZJU 0.8 RS**	**ZJU 1.0 RS**	**ZJU CF**	**Poly-U**	**ZJU 0.8 RS**	**ZJU 1.0 RS**	**ZJU CF**	**Poly-U**
Mean	5.21 (2.50)	5.96 (3.11)	4.70 (3.01)	6.36 (3.23)	2.70 (2.46)	2.42 (1.93)	2.39 (1.52)	3.03 (2.52)
Med.	4.37 (1.81)	4.94 (2.59)	3.28 (2.11)	4.99 (1.40)	1.89 (1.75)	1.61 (1.87)	1.56 (0.90)	2.36 (1.36)
Tri.	4.77 (2.01)	5.11 (2.64)	3.80 (2.30)	5.36 (1.86)	2.19 (2.01)	1.73 (1.66)	1.72 (1.06)	2.66 (1.38)
Best25%	0.99 (0.54)	1.20 (0.92)	1.72 (0.51)	1.50 (0.48)	0.85 (0.75)	0.66 (0.53)	0.80 (0.45)	0.98 (0.38)
Worst25%	8.39 (5.21)	9.10 (7.63)	9.17 (6.67)	9.45 (8.76)	6.91 (6.86)	6.16 (6.17)	6.12 (5.36)	7.34 (7.67)

Table5: Performance Comparison of Various Methods on Cube+ Dataset with Models Trained on NUS-8 Dataset

Method	**Mean**	**Med.**	**Tri.**	**Best25%**	**Worst25%**
GW	3.52	2.55	2.82	0.60	7.98
WP	9.69	7.48	8.56	1.72	20.49
SoG	3.22	2.12	2.44	0.43	7.77
FFCC	2.69	1.89	2.08	0.46	6.31
C5 ($m = 1$)	2.60	1.86	2.10	0.55	5.89
PCC	2.64	2.08	2.23	0.81	5.41
LSCC	2.35	1.77	1.94	0.54	5.16

based methods generally resulted in much poorer performance. The various state-of-the-art learning-based methods had much better performance, with the LSCC method having the smallest angular errors on all the dataset. PCC performs well even with a small network architecture, mainly because the color inputs can effectively characterize the scene's light source, allowing the model to make better predictions.

Table 4 results clearly showed that the KAN universal model outperformed the PCC universal model by a factor over 2, and the performance of the universal model comparing with the individual model is worse by 88% and 28% for PCC and KAN models respectively, indicating that KAN universal model's performance could be quite satisfactory already.

Both Tables 4 and 5 demonstrate that LSCC exhibits superior performance in cross-dataset predictions, particularly for pure color images. Furthermore, LSCC slightly outperforms other learning-based methods in cross-dataset predictions for classical image datasets, with significantly fewer parameters—over four times fewer than those of PCC and approximately 820 times fewer than FFCC, highlighting its efficiency and effectiveness.

Conclusion

Illuminant estimation is crucial for imaging systems, yet pure color images have been understudied. In this study, three new pure color datasets—ZJU Color Fabric, ZJU 0.8 Real Scene, and ZJU 1.0 Real Scene—were developed, covering diverse conditions. Study also introduces the KAN neural networks, which diverges from MLP architectures and achieves high accuracy with fewer parameters and better interpretability. It estimates the chromaticities of the illuminant based on four important color inputs of an image, proposed by [5], including the chromaticities of the maximal, mean, brightest, and darkest pixels in an image.

References

[1] Buchsbaum, G. (1980). A spatial processor model for object colour perception. *Journal of the Franklin Institute*, 310(1), 1-26.

[2] Land, E. H. (1977). The retinex theory of color vision. *Scientific American*, 237(6), 108-129.

[3] Finlayson, G. D., & Trezzi, E. (2004, January). Shades of gray and colour constancy. In *Color and Imaging Conference* (Vol. 12, pp. 37-41). Society of Imaging Science and Technology.

[4] Cheng, D., Prasad, D. K., & Brown, M. S. (2014). Illuminant estimation for color constancy: why spatial-domain methods work and the role of the color distribution. *JOSA A*, 31(5), 1049-1058.

[5] Yue, S., & Wei, M. (2023). Color constancy from a pure color view. *JOSA A*, 40(3), 602-610.

[6] Gehler, P. V., Rother, C., Blake, A., Minka, T., & Sharp, T. (2008, June). Bayesian color constancy revisited. In *2008 IEEE Conference on Computer Vision and Pattern Recognition* (pp. 1-8). IEEE.

[7] Abdelhamed, A., Punnappurath, A. and Brown, M.S., 2021. Leveraging the availability of two cameras for illuminant estimation. In *Proceedings of the IEEE/CVF Conference on Computer Vision and Pattern Recognition* (pp. 6637-6646).

[8] Banić, N., Koščević, K., & Lončarić, S. (2017). Unsupervised learning for color constancy. *arXiv preprint arXiv:1712.00436*.

[9] Hemrit, G., Finlayson, G. D., Gijsenij, A., Gehler, P., Bianco, S., Funt, B., Drew, M., & Shi, L. (2018). Rehabilitating the colorchecker dataset for illuminant estimation. *arXiv preprint arXiv:1805.12262*.

[10] Afifi, M., Barron, J. T., LeGendre, C., Tsai, Y. T., & Bleibel, F. (2021). Cross-camera convolutional color constancy. In *Proceedings of the IEEE/CVF International Conference on Computer Vision* (pp. 1981-1990).

[11] Liu, Z., Wang, Y., Vaidya, S., Ruehle, F., Halverson, J., Soljačić, M., Hou, T. Y., & Tegmark, M. (2024). Kan: Kolmogorov-arnold networks. *arXiv preprint arXiv:2404.19756*.

[12] Paszke, A., Gross, S., Massa, F., Lerer, A., Bradbury, J., Chanan, G., Killeen, T., Lin, Z., Gimelshein, N., Antiga, L., & Desmaison, A. (2019). Pytorch: An imperative style, high-performance deep learning library. *Advances in Neural Information Processing Systems*, 32.

[13] Barron, J. T., & Tsai, Y. T. (2017). Fast fourier color constancy. In *Proceedings of the IEEE conference on computer vision and pattern recognition* (pp. 886-894).

Author Biography

LiangWei Chen received his BS in Optoelectronic Information Science and Engineering from Shenzhen University (2023) and has been a Master student supervised by Professor Ming Ronnier Luo at Zhejiang University since 2023. His research work is on color constancy.